Magnetic separation and characterization of vivianite from digested sewage sludge

Prot, T.; Nguyen, V. H.; Wilfert, P.; Dugulan, A. I.; Goubitz, K.; De Ridder, D. J.; Korving, L.; Rem, P.; Bouderbala, A.; Witkamp, G. J.

DOI
10.1016/j.seppur.2019.05.057

Publication date
2019

Document Version
Final published version

Published in
Separation and Purification Technology

Citation (APA)
Prot, T., Nguyen, V. H., Wilfert, P., Dugulan, A. I., Goubitz, K., De Ridder, D. J., Korving, L., Rem, P., Bouderbala, A., Witkamp, G. J., & van Loosdrecht, M. C. M. (2019). Magnetic separation and characterization of vivianite from digested sewage sludge. *Separation and Purification Technology*, *224*, 564-579. https://doi.org/10.1016/j.seppur.2019.05.057

Separation and Purification Technology 224 (2019) 564–579

Contents lists available at ScienceDirect

Separation and Purification Technology

journal homepage: www.elsevier.com/locate/seppur

Magnetic separation and characterization of vivianite from digested sewage sludge

T. Prot[a,b], V.H. Nguyen[a], P. Wilfert[a,b], A.I. Dugulan[c], K. Goubitz[c], D.J. De Ridder[d], L. Korving[a,*], P. Rem[e], A. Bouderbala[a], G.J. Witkamp[b,f], M.C.M. van Loosdrecht[b]

[a] Wetsus, European Centre Of Excellence for Sustainable Water Technology, Oostergoweg 7, 8911 MA Leeuwarden, the Netherlands
[b] Dept. Biotechnology, Delft University of Technology, Van der Maasweg 9, 2629 HZ Delft, the Netherlands
[c] Fundamental Aspects Mat & Energy Group, Delft University of Technology, Mekelweg 15, 2629 JB Delft, the Netherlands
[d] Sanitary Engineering, Delft University of Technology, Stevinweg 1, 2628 CN Delft, the Netherlands
[e] Resources and Recycling, Delft University of Technology, Stevinweg 1, 2628 CN Delft, the Netherlands
[f] Currently at King Abdullah University of Science and Technology (KAUST), Water Desalination and Reuse Center (WDRC), Division of Biological and Environmental Science and Engineering (BESE), Thuwal 23955-6900, Saudi Arabia

ARTICLE INFO

Keywords:
High gradient magnetic separation
Phosphorus recovery
XRD
Mössbauer spectroscopy
Heavy metals
Fertilizer

ABSTRACT

To prevent eutrophication of surface water, phosphate needs to be removed from sewage. Iron (Fe) dosing is commonly used to achieve this goal either as the main strategy or in support of biological removal. Vivianite ($Fe(II)_3(PO_4)_2 * 8H_2O$) plays a crucial role in capturing the phosphate, and if enough iron is present in the sludge after anaerobic digestion, 70–90% of total phosphorus (P) can be bound in vivianite. Based on its paramagnetism and inspired by technologies used in the mining industry, a magnetic separation procedure has been developed. Two digested sludges from sewage treatment plants using Chemical Phosphorus Removal were processed with a lab-scale Jones magnetic separator with an emphasis on the characterization of the recovered vivianite and the P-rich caustic solution. The recovered fractions were analyzed with various analytical techniques (e.g., ICP-OES, TG-DSC-MS, XRD and Mössbauer spectroscopy). The magnetic separation showed a concentration factor for phosphorus and iron of 2–3. The separated fractions consist of 52–62% of vivianite, 20% of organic matter, less than 10% of quartz and a small quantity of siderite. More than 80% of the P in the recovered vivianite mixture can be released and thus recovered via an alkaline treatment while the resulting iron oxide has the potential to be reused. Moreover, the trace elements in the P-rich caustic solution meet the future legislation for recovered phosphorus salts and are comparable to the usual content in Phosphate rock. The efficiency of the magnetic separation and the advantages of its implementation in WWTP are also discussed in this paper.

1. Introduction

Phosphorus is an essential element for life and is responsible for various functions in both humans and plants. Particularly for plants, it is a major nutrient and hence often spread onto soils in the form of phosphate fertilizer [4]. The source for the phosphate in fertilizer is primarily from mining phosphate rock. This process is environmentally unfriendly, and the resources are becoming depleted whereas human's demand is increasing due to the rise of the population [22]. In parallel with being a necessary nutrient, phosphorus can also cause eutrophication if released in excess into water bodies, obliging Waste Water Treatment Plants (WWTPs) to remove it before discharging the effluents in natural streams [37].

Currently, there are two main methods for advanced phosphorus removal in treatment plants: enhanced biological phosphorus removal (EBPR) and Chemical Phosphorus Removal (CPR). Iron is usually dosed in CPR mainly to remove the phosphorus but it also helps controlling the sulfide production and acts as a coagulant to facilitate sludge dewatering while being a cost-effective chemical. Furthermore, iron can already be present in the influent wastewater depending on its origin, meaning that P could already be partially bound to iron before the dosing step. Iron can also enhance the flocculation/coagulation of suspended particles in wastewater and thereby play a key role in future energy producing WWTP's [32].

It is estimated that 370 kton of phosphorus per year ends up in the sludge of the European WWTP's [31]. By utilizing this resource, up to 20–30% of Europe's fertilizer demand could be met [26]. Hence, various technologies have been developed to serve this purpose, ranging

* Corresponding author.
E-mail address: Leon.Korving@Wetsus.nl (L. Korving).

https://doi.org/10.1016/j.seppur.2019.05.057
Received 1 February 2019; Received in revised form 15 May 2019; Accepted 15 May 2019
Available online 16 May 2019
1383-5866/

from the direct use of sewage sludge on farmland to more advanced methods such as recovery from incinerated sewage sludge ash or recovery as struvite [7]. There have not been many technologies proposed serving treatment plants using CPR without the requirements for incineration. Incineration is often disapproved by the public and capital intensive as it requires expensive infrastructures.

In WWTP's dosing iron, several researchers reported the presence of the iron phosphate mineral vivianite ($Fe_3(PO_4)_2{\cdot}8H_2O$). Frossard et al. [11] discovered sand-sized to silt-sized vivianite in sludge while [27] observed it in dried sewage sludge. Nriagu and Dell [19] evaluated that vivianite was the most thermodynamically stable FeP mineral in reductive environments, such as in sediments and sludge. More importantly, vivianite should form preferably over struvite during sludge digestion according to thermodynamic evaluations. Wilfert et al. [33] observed this in two WWTP's where vivianite was found as the dominant FeP mineral in the digested sludge. In line with the findings of [20], this study also showed that Fe(III) compounds are reduced and transformed to vivianite in the activated sludge tanks even though Fe (III) was dosed. Additionally, [34] suggested that after digestion between 70 and 90% of the total amount of P present in sludge can be bound to vivianite provided the dosing of iron is high enough.

With such a high fraction of P potentially present as vivianite, there is an opportunity to recover P from sludge through extraction of vivianite. It is especially interesting considering that only 10–50% of the total P in the influent can be recovered via struvite precipitation [5]. Interestingly, vivianite is a paramagnetic mineral with a magnetic susceptibility varying from 0.8 to $1.7{\cdot}10^{-6}\,m^3/kg$ [16]. Apart from some other Fe bearing species, vivianite is the only main paramagnetic compound in sludge. Magnetic separation would, therefore, provide a selective way to recover vivianite from sludge.

Seitz et al. [27], already designed an experimental set-up to separate vivianite from dried sludge powder using magnetic attraction. There are also other devices from the mining industry like the Frantz separator that were used to extract magnetic fractions from streams but never tested to extract vivianite from sludge. These separators can only work with dry materials and the separation of vivianite from sludge was not achieved with high efficiency [2]. Another device having the potential for this extraction process is the Jones separator, a high-intensity magnetic separator that can be used directly with wet sludge [36]. In this study, a device mimicking the working mechanism of the Jones separator was used to extract vivianite from sludge. The objective of this study was to provide the proof of principle that this technique can work and to investigate the composition of the extracted fraction. The magnetic separation of ferrite sludge from wastewater has already been studied earlier [1] but is different from the technique studied here. Vivianite is paramagnetic and not ferromagnetic which makes its separation more challenging.

2. Materials and methods

2.1. WWTP's and sample handling

For this research, digested sludges from 2 WWTP's have been used. One was sampled in Dokhaven (The Netherlands) and the other in Espoo (Finland). Both plants rely on CPR by dosing iron salts in different molar ratios to phosphate, which has an impact on the quantity of vivianite formed. After sampling, the sludges were kept in polyethylene bottles of 1L and stored in a 4 °C fridge. Before any tests or analyses, the sludges were sieved with a 1 mm sieve to remove any large particles in the sludge. No particular precautions were taken to maintain anaerobicity of the feed samples considering that the sludge buffers oxygen and oxidation of vivianite should be slow in these conditions. A relatively pure (~95% as determined with ICP-OES), vivianite scaling found in a heat exchanger from the WWTP of Venlo (The Netherlands) has been used as comparison during the study. More information about the sieved and non-sieved sludges can be found in Appendix A.

2.2. Magnetic separation and P release

2.2.1. Definitions

In this study, the initial mix from which the product is extracted is called the feed. The magnetic fraction containing the vivianite is the concentrate, while the non-wanted part is the tailing. The grade is the purity of the concentrate in terms of dry weight, and the recovery expresses the amount of a compound ending up in the concentrate compared to its quantity in the feed. The yield is defined as the quantity of concentrate compared to the feed in term of dry weight.

2.2.2. Device description

A lab-scale replicate of the separator (μ-Jones) has been designed to investigate the application of this system to sludge. The μ-Jones consists of two steel plates with seven vertical 4 cm-high/1.5 mm long teeth. The ridges are 2 mm away from each other and made magnetic with 2 * 3 Nd-Fe-B permanent magnets of ~1.3 T (creating a magnetic field of ~1.3 T on the ridge and ~0.3 T in-between the teeth)(Fig. 1). The μ-Jones is put in water until the teeth are entirely submerged to increase the contact time between the teeth and the sludge. An aluminum tray was designed to collect the solids as soon as they are released from the teeth. Further information about the working principle of a full-scale Jones separator can be found in [36].

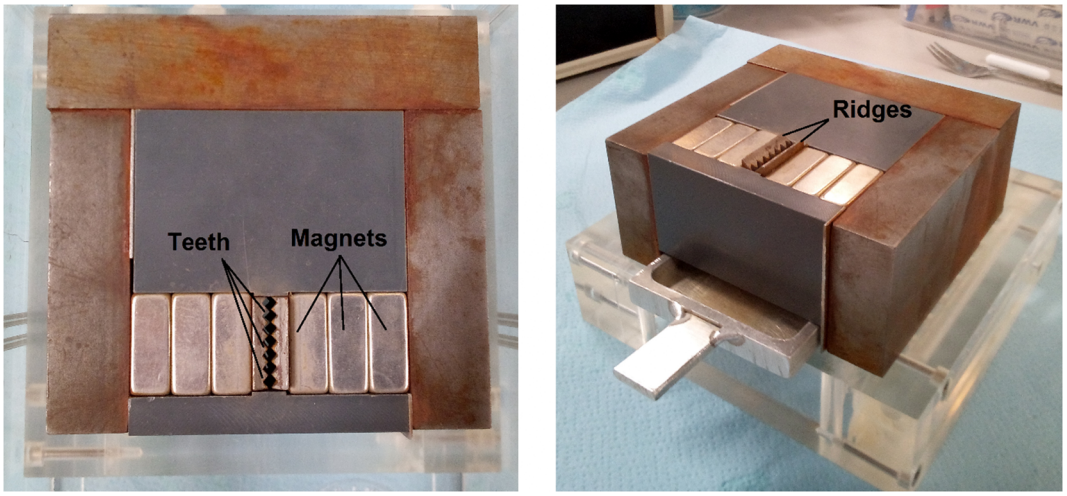

Fig. 1. μ-Jones top view (left) and side view (right).

2.2.3. Separation protocol

The sludge is continuously mixed for homogenization, and 20 mL/min are pumped on the teeth (Appendix B). The sludge from Finland was pumped for 30 s and the sludge from the Netherlands 45 s to obtain a similar quantity of concentrate because the amount of iron in the Finish sludge is higher. To wash away a maximum of non-magnetic residues stuck in the teeth (mainly organic matter), Milli-Q water (MQW) is pumped at 20 mL/min for 30 s. Finally, the μ-Jones is removed from the water, and a stronger flow of MQW is sent through the teeth with a squeeze bottle to free all the material attached to the ridges.

As a post-treatment, the wet concentrate was introduced in 50 mL tubes to be centrifuged at 3750 rpm for 30 min. The pellets were then vacuum-dried at 30 °C for 1–2 days. Around 250 mL (Finnish) and 500 mL (Dutch) of sieved sludge was necessary to separate 1 g of dried material. Feed samples were directly poured into a petri dish after sieving and vacuum dried at 30 °C. All the materials (including the scaling) were then ground and stored in 15 mL plastic tubes without precaution toward exposure to oxygen or light. Once extracted from the sludge, vivianite is not protected anymore and can easily be oxidized [15,3].

2.2.4. Release of phosphorus from vivianite

An alkaline treatment was used to release P from vivianite. 20 mg of concentrate was introduced in 10 mL of Ultratrace water (Sigma-Aldrich) under stirring, and 0.2 mL of 7.5 M ultratrace NaOH was added giving an OH^-/Fe molar ratio excess of 5–10. The release solution is let to stir for 2 h to be sure that the reaction is over. A change of color can be observed from transparent to the characteristic rust brown of Fe $(OH)_3$. The precipitates were removed by 0.45 μm filtration, and the filtrate was analyzed for elemental composition.

2.3. Analyses

2.3.1. XRD

The sample was filled in a 0.7 mm glass capillary and tamped so the solid settles. No precautions toward oxygen-free conditions have been taken. Just before measurement the capillaries were sealed with a burner and mounted in a sample holder. The device used was a PANalytical ẊPert PRO diffractometer with Cu-Ka radiation (5–80° 2θ, step size 0.008°). The fitting was realized with the software Origin Pro 9.

2.3.2. SEM-EDX

The apparatus is a JEOL JSM-6480 LV scanning electron microscope (SEM) equipped with an Oxford Instruments x-act SDD energy dispersive x-ray (EDX) spectrometer. The accelerating voltage used is 15.00 kV for a working distance of 10 mm. A 10 nm-layer of gold is deposited on the sample with a JEOL JFC-1200 fine coater to make the surface electrically conductive. The softwares used are JEOL SEM Control User Interface for the SEM and Oxford Instruments Aztec for the EDX data processing.

2.3.3. Mössbauer spectroscopy

The sample weight was adjusted to have 15 mg of Fe/cm^2. Transmission ^{57}Fe Mössbauer absorption spectra were collected at 300 K and 77 K with a conventional constant-acceleration spectrometer using a ^{57}Co (Rh) source. Velocity calibration was carried out using an α-Fe foil. The Mössbauer spectra were fitted using the Mosswinn 4.0 program [13].

2.3.4. TG-DSC-MS

To evaluate the vivianite and the organic share in the samples, Thermo Gravimetry equipped with Differential Scanning Calorimetry, and a Mass Spectrometer (TG-DSC-MS) were used. The apparatus is a STA 449 F3 Jupiter for the simultaneous TG-DTA/DSC and QMS 403C Aëolos for the MS detector, both from NETZSCH Gerätebau GmbH. 40 mg of sample is introduced in the oven which follows a continuous heating ramp of 10 °C/min from 40 °C until 550 °C, under Argon atmosphere.

2.3.5. Digestion

All the solid samples have been destroyed by microwave digestion to perform liquid analyses. The digestion takes place in an Ethos Easy from Milestone with an SK-15 High-Pressure Rotor. 10 mg of solid are introduced in a Teflon vessel in which 10 mL of ultrapure HNO_3 (64.5–70.5% from VWR Chemicals) is poured. The digester is set to reach 200 °C in 15 min, run at this temperature for 15 min and to cool down for 1 h.

2.3.6. ICP-OES/MS

The elemental composition was measured via Inductively Coupled Plasma (Perkin Elmer, type Optima 5300 DV) with an Optical Emission Spectroscopy as detector (ICP-OES). The device was equipped with an Autosampler, Perkin Elmer, type ESI-SC-4 DX fast, and the data were processed with the software Perkin Elmer WinLab32. The rinse and internal standard solution were respectively 2% of HNO_3 and 10 mg/L of Yttrium.

ICP-OES doesn't allow to determine concentrations < 0.05 ppm, so another ICP equipped with a Mass Spectrometer detector (ICP-MS) was also used. The device is a PlasmaQuant MS from Analytik-Jena and was used with three different analytical methods, depending on the element studied: with He (120 mL/min), with H_2 (80 mL/min) or without gas (ng). Y and In were used as internal standard in both gas mode whereas Sc and Y were used in no gas mode.

The samples from the P release experiments weren't digested before analysis but only filtered with a 0.45 μm filter to remove the precipitates. More details about the ICP-MS method can be found in Appendix D.

3. Results

The magnetic separation of vivianite from digested sludge was performed, and the feeds and concentrates were analyzed to evaluate the separation. A relatively pure vivianite scaling sample from a WWTP plant in Venlo was used as reference material. The names and description of the samples are presented in Table 1.

3.1. Solid analysis

3.1.1. XRD

Vivianite was detected in all five samples described in Table 1 and

Table 1
Sample names and description.

Sample name	Description
Feed NL	Sieved digested sludge from Dokhaven (Netherlands) with a molar Fe/P ratio of 0.99
Feed FI	Sieved digested sludge from Espoo (Finland) with a molar Fe/P ratio of 2.19
Conc. NL	Magnetic fraction (concentrate) obtained from the processing of Feed NL
Conc. FI	Magnetic fraction (concentrate) obtained from the processing of Feed FI
Scaling	Vivianite scaling of a purity > 95% of vivianite harvested in Venlo (Netherlands). This scaling is used as reference for "pure" vivianite produced in sewage sludge

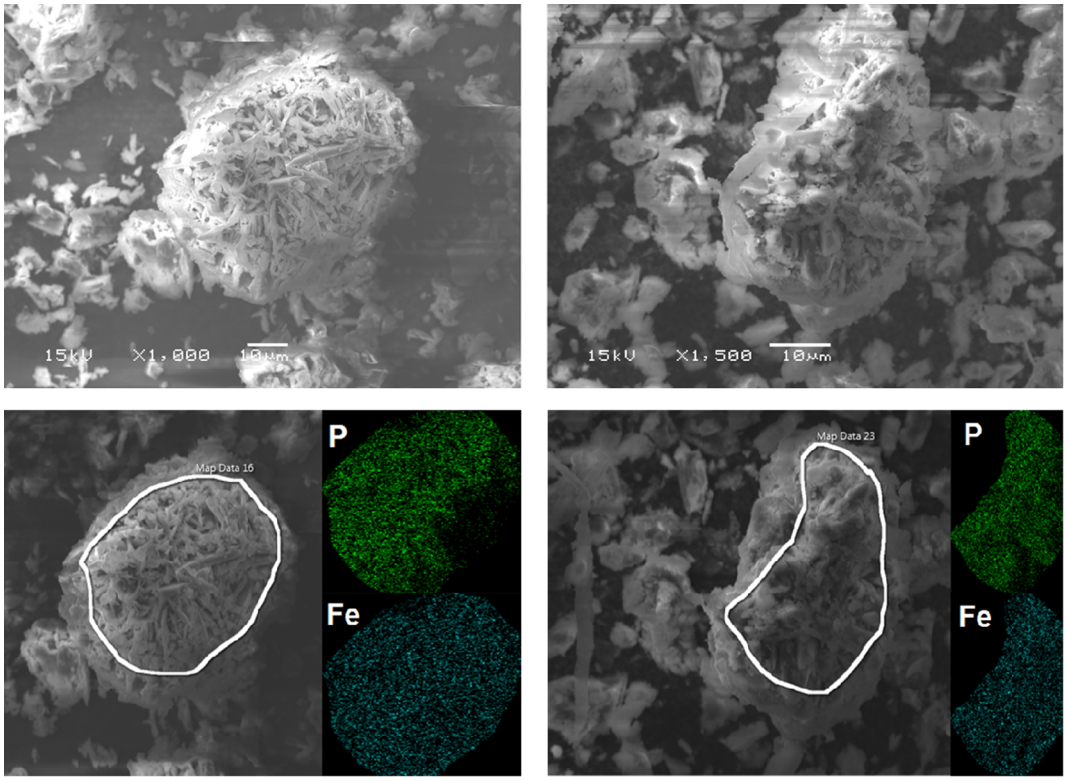

Fig. 2. SEM pictures (top) and corresponding EDX maps (bottom) of the concentrates from Finland (left) and the Netherlands (right).

was the only crystalline phase observed in all cases except for Feed NL (presence of quartz detected). While all the peaks could be assigned in the diffractograms obtained for the scaling and Conc. FI, one, three and four peaks remain unidentified for Conc. NL, Feed NL, and Feed FI, respectively. The bump between 15 and 40° that is usually considered to be amorphous material is absent for the concentrates and the scaling. The diffractograms can be found in Appendix F.

3.1.2. SEM-EDX

SEM-EDX showed that Fe and P were not homogeneously distributed but clustered in specific overlapping places presenting sheet or needle-shaped crystals (5–15 µm) agglomerated into bigger particles (30–100 µm) (Fig. 2). All the particles had a Fe/P ratio of 1.2–1.9, in the range of the one of vivianite (Table 2). Mg, Ca and Al were homogeneously distributed in the sample while S and Si were forming small clusters.

3.1.3. Mössbauer spectroscopy

In Table 3, Fe^{3+} stands for oxidized iron either in the vivianite structure or as another Fe (III) species. Fe^{II} stands for low-spin iron compounds (typically pyrite). In the crystalline structure of vivianite, Fe^{2+} ions can occupy three positions, always in the center of octahedrons formed by water molecules and oxygen atoms. Two positions are equivalent and named Fe^{2+} Vivianite B in Table 3 while the third is unique and called Fe^{2+} Vivianite A [12]. Other crystalline Fe phases weren't identified.

Table 2
Molar ratio of the Fe/P overlapping particles found in the samples (EDX results).

	Scaling	Feed NL	Feed FI	Conc. NL	Conc. FI
Molar Fe/P ratio	1.8	1.2	1.6	1.4	1.9

3.1.4. TG-DSC-MS

The TG analysis of the scaling presented a weight decrease of 25% before 200 °C while 5% is lost between 200 °C and 550 °C. The other samples presented two weight decreases, the first one being steeper for the concentrates than for feed samples. The temperature intervals for the loss of water and CO_2 (blue and orange curves in Fig. 4) are slightly different for each sample (Table 4). Based on the MS signal and the results for the scaling, the first weight decrease can be attributed to the evaporation or 7 of the 8 H_2O of vivianite while the second decrease should account for the last H_2O, the organic fraction and other unidentified minor phases.

3.2. Elemental composition: ICP-OES/MS

The elemental composition of all samples has been determined after microwave digestion. For both feeds, the major elements detected were Fe, P and Ca, with twice as much Fe in FI Feed than NL Feed due to the larger Fe dosing. The quantity of Fe and P increased by a factor 2–3 after separation while the other elements' share was reduced (Table 5).

ICP-MS was used in complement of ICP-OES to reach lower concentrations. The limit of quantification (LOQ) was established by setting a threshold of 20% to the relative standard deviation (RSD) of the calibration curve for each element [30]. Only results above the LOQ are presented in Table 6. For these analyses the device encountered analytical problems measuring Si, S, K, Ca and Ti. As observed by ICP-OES, most elements are reduced in concentration after magnetic separation.

After the alkaline release of P from the concentrates and filtration, only 4 elements can be detected in the filtrate by ICP-OES (Table 7). This result is confirmed by the small number of elements detected by ICP-MS in further experiments (Table 8). The device encountered problems measuring Si, S, K, Ca and Ti for these measurements.

Table 3
Mössbauer data for the 5 samples at 300 K.

Sample	*T (K)*	*IS (mm·s^{-1})*	*QS (mm·s^{-1})*	*Hyperfine field (T)*	*Γ (mm·s^{-1})*	*Phase*	*Spectral contribution (%)*
Scaling	300	0.33	0.88	-	0.54	Fe^{3+}	32
		1.22	2.40	–	0.36	Fe^{2+} Vivianite A	27
		1.22	2.96	–	0.36	Fe^{2+} Vivianite B	41
NL conc.	300	0.34	0.88	–	0.49	Fe^{3+}/Fe^{II}	35
		1.26	2.35	–	0.39	Fe^{2+} Vivianite A	25
		1.23	2.95	–	0.39	Fe^{2+} Vivianite B	40
FI conc.	300	0.38	0.82	–	0.53	Fe^{3+}/Fe^{II}	70
		1.25	2.09	–	0.39	Fe^{2+} Vivianite A	16
		1.19	2.95	–	0.39	Fe^{2+} Vivianite B	14
NL feed	300	0.36	0.85	–	0.53	Fe^{3+}/Fe^{II}	66
		1.27	2.31	–	0.31	Fe^{2+} Vivianite A	13
		1.22	2.97	–	0.31	Fe^{2+} Vivianite B	21
FI feed	300	0.38	0.87	–	0.57	Fe^{3+}/Fe^{II}	61
		1.21	1.99	–	0.43	Fe^{2+} Vivianite A	27
		1.14	2.81	–	0.43	Fe^{2+} Vivianite B	12

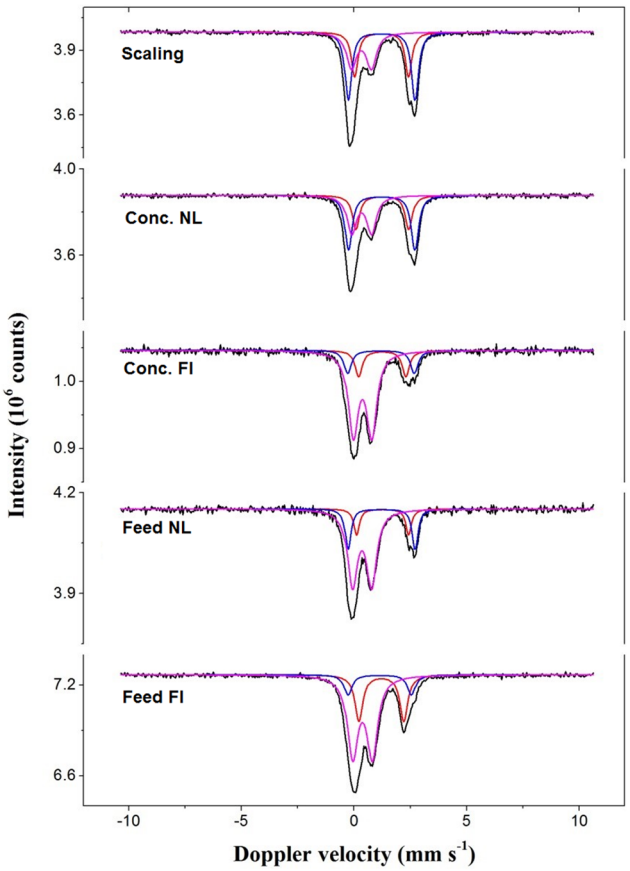

Fig. 3. Mössbauer spectra obtained at 300 K with the signal of Fe^{3+}/Fe^{II} in pink, Fe^{2+}Vivianite A in red, $Fe2^{+}$ Vivianite B in blue and the sum of the spectrum in black. (For interpretation of the references to color in this figure legend, the reader is referred to the web version of this article.)

4. Discussion

The objective of this project was to prove that magnetic extraction of vivianite from sludge is possible and selective by means of a lab scale magnetic separator that mimics the working principle of large scale wet magnetic separators. As a proof of concept study, a pure product rather than a high yield was sought in order to selectively extract vivianite to be able to study and understand how vivianite is present in digested sewage sludge. Three main points will be discussed in the following section:

- The magnetic separation performances
- The composition of the magnetic concentrate in terms of vivianite content and side products.
- The valorization possibilities of the concentrate with an emphasis on its transformation into a fertilizing material

The samples names and description are indicated in Table 1.

To evaluate the potential of the magnetic separation, it is interesting to compare the composition of the magnetic fraction to the digested sludge, before separation. The vivianite content in the magnetic concentrates was reliably estimated with ICP-OES and TG-DSC-MS (see further in the discussion). Mössbauer spectroscopy is unable to differentiate the fraction of oxidized vivianite from other Fe^{3+} bearing compounds present in sludge. The samples were exposed to oxygen during the separation and sampling handling, resulting in some oxidation of the vivianite. Therefore, in this case, Mössbauer spectroscopy underestimated the vivianite content and gives the minimum rather than the exact content. Furthermore, the maximum vivianite content can be obtained by hypothesizing that all the P measured by ICP-OES in the samples are present as vivianite. A combination of Mössbauer spectroscopy and ICP-OES gives a range of vivianite content in the digested sludge (Table 9). Earlier, more detailed studies on the vivianite content of the same sludges [34] estimated the phosphorus present as vivianite at 65% and 85% of the total phosphorus (average value from their measurements) in NL Feed and FI Feed, respectively. Based on the elemental composition of these sludge in Table 5, the vivianite weight content can be estimated at 20% for both sludges. This suggests that the magnetic separation concentrates the vivianite by a factor 2–3, which is promising at this stage. The magnetic separation also reduces the organic content from 40% to 20% (Table 9). The remaining could be the organic matter that seems to trap the vivianite crystals, as suggested by Fig. 2 and Frossard et al. [11]. The persistence of quartz even after magnetic separation is surprising considering that quartz is not paramagnetic. It could act as a nucleation center for vivianite, and may, therefore, be present in its structure, and be extracted with it.

Since the concentration of heavy metals is relevant for the valorization of the magnetic concentrate, we studied the concentration factor of heavy metals during the separation. Our study shows that the magnetic separation reduces the heavy metal to phosphorus ratio (Appendix E). However, this is not the case for the cations Mn, Ni, Mg and Cu that remained similar or increased. The authors see two possible explanations for the persistence of these elements in the magnetic fraction: they could form other magnetic compounds than vivianite, or substitute

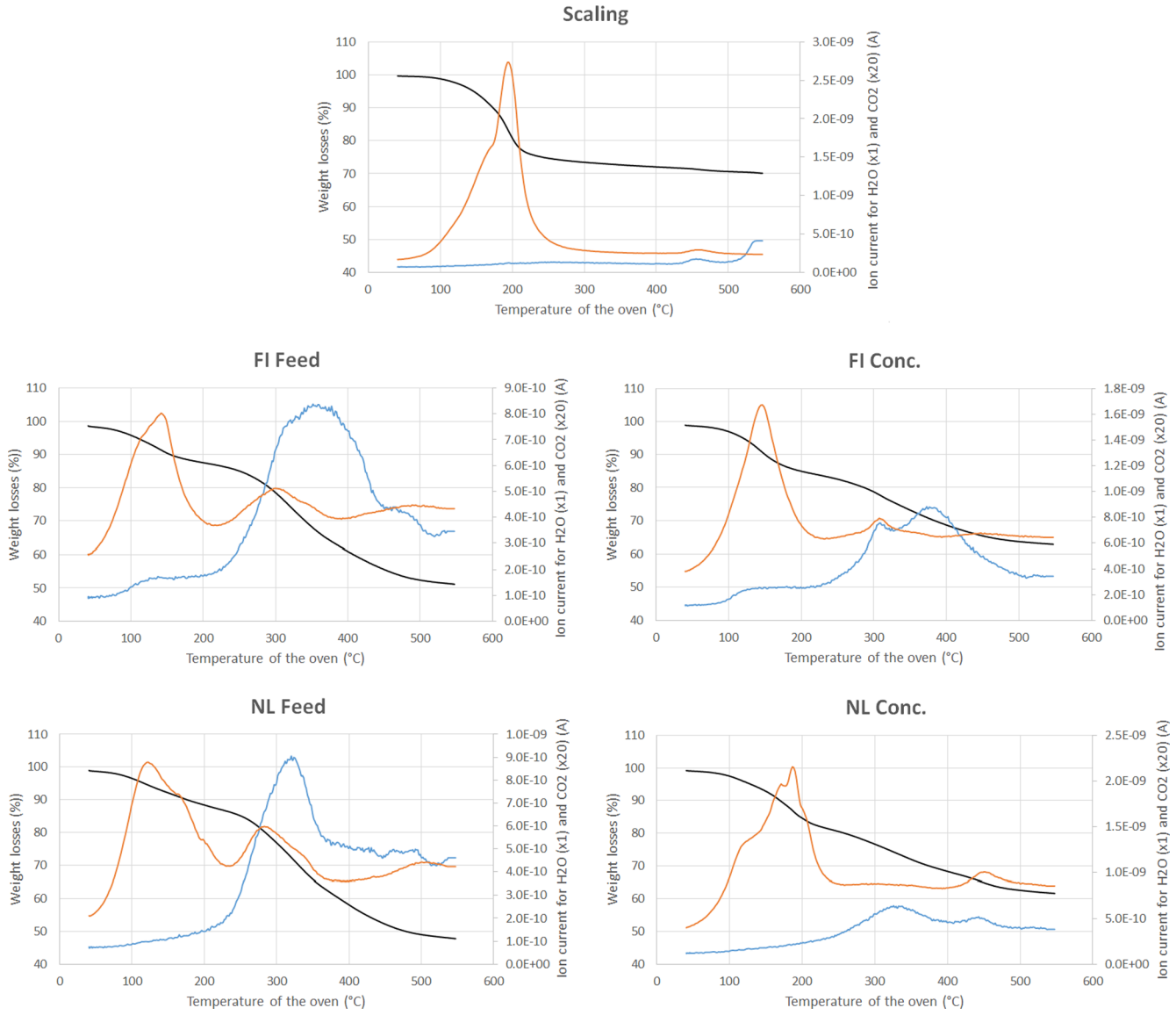

Fig. 4. TG-DSC-MS spectra for the scaling, both feeds, and concentrates. In black the weight losses, in orange the Mass Detector signal for H_2O and in blue for CO_2. (For interpretation of the references to color in this figure legend, the reader is referred to the web version of this article.)

Table 4
Weight losses during the 1st and the 2nd decrease in TG analysis (after vacuum oven drying).

Sample	1st decrease (% of weight lost)	2nd decrease (% of weight lost)
Scaling	25 (40–220 °C)	5 (220–550 °C)
Feed FI	10 (40–200 °C)	36 (200–550 °C)
Feed NL	12 (40–220 °C)	40 (220–550 °C)
Conc. FI	14 (40–200 °C)	23 (200–550 °C)
Conc. NL	17 (40–200 °C)	20 (200–550 °C)

Fe^{2+} in the structure of vivianite. Vivianite is known to have a structure allowing substitution of its Fe^{2+} atoms by other divalent cations [24,29]. At ambient temperature, 2 Fe^{2+} occupy the 2 octahedral sites B while 1 Fe^{2+} occupies the octahedral site A. Therefore, the ratio (Fe^{2+} Vivianite B / Fe^{2+} Vivianite A) given by Mössbauer should be 2 for pure vivianite [15,17]. Divalent cations substitute preferentially in site B, decreasing this ratio [14]. The samples have ratios < 2 suggesting the presence of impurities (Table 10). This ratio is an interesting indicator to assess the purity of the vivianite, but oxidation of the mineral complicates the evaluation. Rouzies and Millet [25] and McCammon et al. [15] consider that oxidation happens preferentially in site A which should then increase the ratio. The antagonist effects of the oxidation and the impurities make a quantitative approach impossible in the case of samples that were exposed to air, as was the case in this study.

A deeper characterization of the magnetic fractions has been realized to assess the purity of the product. First of all, vivianite was clearly identified in the magnetic concentrates by Mössbauer spectroscopy and XRD. Crystals showing a Fe/P ratio close to 1.5 (as in pure vivianite) were also observed by SEM-EDX (Table 2). Moreover, the morphology of these crystals as in Fig. 2 agrees with the sheet/needle-shaped appearance of vivianite already reported by several authors [38,29].

The quantification of vivianite is complicated and, therefore, ICP-OES, TG-DSC-MS and Mössbauer spectroscopy were used together to give the best result possible (Table 11). A first estimate of the vivianite content can be made based on the elemental composition (ICP-OES) by hypothesizing that all the phosphorus is bound to vivianite in these samples. It seems like a reasonable assumption since vivianite should be the major (if not the only) magnetic P-compound in sludge. Additionally, TG-DSC-MS was used. This method is based on the dehydration process of vivianite, that loses its 8 crystal water with

Table 5
Elemental composition of the feeds, concentrates and scaling measured by ICP-OES.

g/kg of dry matter	Fe	P	Ca	Mg	Al	S	K	Zn	Si	Cu	Na	Mn
FI Feed	120.3 ± 0.5	28.4 ± 0.1	26.7 ± 0.6	4.0 ± 0.1	6.1 ± 0.1	8.6 ± 0.1	10.8 ± 0.3	0.8*	7.9 ± 0.1	nd	nd	nd
FI Conc.	236.2*	64.6 ± 0.7	17.14 ± 0.6	2.8 ± 0.1	4.6 ± 0.1	6.0 ± 0.8	2.0*	0.5*	5.5 ± 0.2	1.0*	nd	nd
NL Feed	63.9 ± 0.1	37.4 ± 0.6	36.2 ± 0.7	3.4 ± 0.1	6.0 ± 0.1	20.9 ± 0.2	10.3 ± 0.1	1.3 ± 0.1	7.00 ± 0.1	0.7 ± 0.1	7.2*	nd
NL Conc.	195.2*	77.21 ± 0.8	20.0 ± 0.4	7.50 ± 0.1	4.62 ± 0.1	9.6 ± 0.4	1.8*	0.7*	5.56 ± 0.1	0.7*	nd	2.4*
Scaling	308.0*	119.0 ± 2.2	9.5 ± 0.5	10.8 ± 0.1	nd	1.70 ± 0.8	nd	nd	nd	nd	nd	3.0 ± 0.1

nd: not detected because the concentration was below the LOQ of the device for both duplicates.
* One of the duplicate is out of range (high or low).

Table 6
Elemental composition of the feeds, concentrates and scaling measured by ICP-MS.

Sample	Weight content (mg element/kg of dry matter)									
	Cr	As	La	Li	Mg	Al	Mn	Co	Ni	Cu
FI Feed	33.1 ± 0.6	8.7 ± 0.5	30.1 ± 0.3	3.6 ± 0.1	> 790	> 790	252.0 ± 0.5	8.8 ± 0.1	33.3 ± 0.3	378.3 ± 4.2
FI Conc.	25.1 ± 0.5	7.7 ± 0.7	24.4 ± 0.3	3.1 ± 0.2	> 790	> 790	414.3 ± 3.01	9.2 ± 0.1	398.2 ± 1.3	> 790
NL Feed	50.7 ± 0.7	40.1 ± 1.2	9.5 ± 0.1	3.9 ± 0.2	> 790	> 790	634.5 ± 4.6	6.1 ± 0.1	42.2 ± 0.5	685.6 ± 10.9
NL Conc.	59.7 ± 1.7	17.9 ± 0.4	7.0 ± 0.1	3.8 ± 0.2	> 782	> 782	> 782	8.5 ± 0.1	90.6 ± 0.6	710.0 ± 4.5
Scaling	nd	nd	nd	nd	> 782	297.1 ± 0.8	> 782	31.7 ± 0.4	78.6 ± 0.5	17.1 ± 1.5

Sample	Weight content (mg element/kg of dry matter)								
	Zn	Mo	Ag	Sn	Ba	Pb	Na	Rb	Ce
FI Feed	725.1 ± 10.8	6.0 ± 0.1	2.8 ± 0.1	27.3 ± 0.2	114.2 ± 0.6	15.4 ± 0.1	> 790	10.6 ± 0.1	74.8 ± 0.7
FI Conc.	414.2 ± 0.9	4.1 ± 0.1	nd	18.3 ± 0.1	94.2 ± 0.7	8.2 ± 0.1	nd	6.6 ± 0.2	51.3 ± 0.4
NL Feed	> 790	11.8 ± 0.1	7.0 ± 0.2	25.5 ± 0.2	400.7 ± 1.2	113.1 ± 1.8	> 790	7.9 ± 0.2	13.1 ± 0.2
NL Conc.	648.1 ± 7.0	5.6 ± 0.1	3.3 ± 0.3	17.7 ± 0.2	239.8 ± 1.4	81.5 ± 0.6	239.3 ± 40.5	5.0 ± 0.2	11.4 ± 0.1
Scaling	267.7 ± 2.0	nd	nd	nd	nd	3.3 ± 0.1	nd	nd	nd

nd: no data, meaning below LOQ for both replicates.

temperature increase. The vivianite scaling used as a reference for pure vivianite (Table 1) indicates that 7 of its 8 crystal water evaporate in the temperature range 40–200 °C (Fig. 4). The vivianite content in the concentrates is estimated by matching the weight decrease in this temperature range to the loss of 7 water molecules (Table 4). In complement, Mössbauer spectroscopy was used. It can detect the Fe^{2+} ions of vivianite but is unable to quantify them after they oxidize to Fe^{3+}, even though they are still present in the structure of vivianite. This is because the signal of Fe^{3+} in vivianite overlaps with other oxidized Fe phases and low-spin iron like in pyrite [18] and cannot be isolated. Therefore, only the contribution of Fe^{2+} can be taken into account to estimate the vivianite content, this giving a conservative estimate for the vivianite content. No precaution toward oxidation has been taken during magnetic separation and sample handling, and therefore the Fe^{3+} content in any recovered vivianite will not be negligible explaining the low vivianite content obtained with Mössbauer in Table 11. ICP-OES and TG-DSC-MS seem fit to estimate the vivianite content in the magnetic fraction while Mössbauer spectroscopy requires extreme precaution toward oxidation to be reliable.

Vivianite accounts for 50–60% of the weight of the magnetic fractions, so 40–50% are left to determine. Organic matter, quartz and carbonates (likely to be siderite $FeCO_3$) were also found and their estimated content are listed in Table 12. Organic matter has been quantified by TG-DSC-MS since it should lead to mass loss due to pyrolysis and gasification before 550 °C (responsible for the second weight drop in Table 4). The quartz content was considered to be equal to the residue after microwave digestion. SEM EDX confirmed this residue contained mainly silica and oxygen. The carbonate quantity was estimated based on the CO2 release from the sample after acid addition to the sample. Methods and results are detailed in Appendix C.

Table 7
Elemental composition of the release solution for both concentrates measured by ICP-OES.

Sample	Weight content (g solubilized element/kg of dry matter)			
	Al	P	S	Si
FI Conc. release	1.84 ± 0.12	59.67 ± 4.64	5.04 ± 0.68	0.96*
NL Conc. release	1.73 ± 0.18	69.93 ± 5.54	6.70 ± 0.54	nd

nd: no data, meaning below LOQ for both replicates.
* The second replicate is below the LOQ of the device.

The Fe content in the magnetic fraction is high compared to the phosphorus content (Table 5) and the presence of vivianite cannot alone explain it. Therefore, other Fe species must have been extracted together with vivianite. No other Fe compound was positively identified by XRD or Mössbauer, indicating a low content, a small size or/and an amorphous nature of these Fe compounds. The carbonates found in the magnetic fractions are likely to be $FeCO_3$ (siderite) (Appendix C); not only is it a magnetic specie [10] but it is also the possible reason for the interference observed with Mössbauer spectroscopy (see explanation below Table 10). Pyrite, another magnetic compound, can potentially be present in the magnetic fraction and could account for 3–5% of the dried weight if we consider that the sulfur quantified by ICP-OES is present in the form FeS_2. SEM-EDX also revealed some Fe/S clusters (results not showed) which support this hypothesis. As mentioned above, pyrite is a low-spin Fe and cannot be distinguished from Fe^{3+} species by Mössbauer, explaining why it has not been identified with certainty. Other Fe-species like FeOH's should be present in the

Table 8
Elemental composition of the release solution for both concentrates measured by ICP-MS.

Sample	Weight content (mg solubilized element/kg dry matter)							
	As	Mn	Ni	Cu	Zn	Mo	Sn	Fe
FI Conc. release	3.18 ± 0.08	2.66 ± 0.34	90.51 ± 1.24	196.16 ± 6.85	24.76 ± 2.52	2.20 ± 0.05	10.58 ± 0.74	281.49 ± 23.42
NL Conc. release	12.98 ± 0.68	8.76 ± 0.32	12.48 ± 0.06	113.59 ± 3.44	34.21 ± 2.54	2.76 ± 0.04	9.09 ± 0.48	183.77 ± 50.13

Table 9
Vivianite, organics and quartz content of the feeds and concentrates (processed data from Tables 3–5 and C2).

% of dried matter	Vivianite*	Organics**	Quartz**
FI Feed	6.9–23.0	39 ± 2	8
FI Conc.	52.3 ± 0.6	20 ± 2	8
NL Feed	6.6–30.2	42 ± 2	4
NL Conc.	62.5 ± 0.7	19 ± 2	7

* For the concentrates, the content has been determined with ICP-OES assuming that all the P is bound to vivianite which should be the major (if not the only) magnetic P-specie in the sample. For the Feeds, this hypothesis is not applicable considering the diversity of P compounds in sludge (CaP, organic P…). Therefore, a range is given with the minimum determined by Mössbauer and the maximum by ICP-OES.

** Details of the determination of the content stand in Appendix C.

Table 10
Spectral contribution of both Fe^{2+} sites of vivianite at 300 K and site ratio (processed data from Table 3).

Sample	Fe^{2+} Vivianite A (%)	Fe^{2+} Vivianite B (%)	Ratio B/A
NL Conc.	25	40	1.6
FI Conc.	9*	14	1.6
NL Feed	13	21	1.6
FI Feed	7*	12	1.7

* The QS of Vivianite A (Table 3) is lower than it should (~2.1 instead of ~2.4 mm/s) for these samples indicating a probable interference with the siderite (QS ~ 1.8 mm/s) present as well. Therefore, the contribution of siderite (calculated further in the discussion) is deducted from this signal, giving a spectral contribution of 9% (instead of 16%) and 7% (instead of 27%) for FI Conc. and FI Feed, respectively.

Table 11
Vivianite content in the concentrates estimated with different analytical methods (processed data from Tables 3–5).

Content (weight % of dried matter)	Conc. NL	Conc. FI
ICP-OES	62.5 ± 0.7	52.3 ± 0.6
TG-DSC-MS	68 ± 8	56 ± 8
Mössbauer	38.4 ± 0.9	16.4 ± 0.3*

* See explanation below Table 10.

magnetic fraction to account for the rest of Fe^{3+} detected by Mössbauer.

In conclusion, the magnetic fractions contain organic matter (20%), quartz (7–8%), pyrite (3–5%), siderite (0.3–3%) and other not identified compounds. Most importantly, the vivianite content is estimated to be around 50% of the concentrate, showing the feasibility to concentrate vivianite magnetically, albeit that further work needs to be done to improve the purity of the concentrate, and the yield.

Once vivianite is recovered from sludge, several valorizations may be foreseen. If a high-grade concentrate could be obtained, high-value applications could be considered. Using vivianite in art to create pigments or as a component in the lithium-ion batteries are two such high-value possibilities [3,21]. Several studies have already investigated the direct use of vivianite as a slow P-release fertilizer and its advantage for Fe-poor soils [9,23]. However, they were working with natural vivianite and not vivianite from sewage, which might bear heavy metals, possibly limiting a direct use. On the other hand, their presence could also be beneficial for some plants requiring micronutrients like Cu or Zn.

Table 12
Organic matter, $FeCO_3$ and quartz content measured in both magnetic concentrates.

Content (weight % of dried matter)	Organic matter*	$FeCO_3$*	Quartz*
FI Conc.	20 ± 2	3.33 ± 0.16	8 ± 1
NL Conc.	19 ± 2	0.26 ± 0.02	7 ± 1

* Details of the determination of the content is in Appendix C.

If the purity of the concentrate is too low for direct application, a post-treatment is required to crack vivianite and recover the P and the Fe. With this objective, the magnetic concentrate was put in an alkaline solution (Section 2.2.4) which broke down the vivianite, released P in solution, while Fe and the other heavy metal precipitated as hydroxides. The precipitates were filtered out and around 90% of the P from vivianite was recovered in the liquid fraction.

The heavy metal concentrations in these P-rich solutions were in line with the future legislation on recovered phosphorus salts and the common concentration in P-rock for most of the elements considered (except for Ni in FI Conc. and As in NL Conc.) (Table 13). The analytical method for Cd and Cr needs to be further developed to lower the limit of quantification. Concentrations of organic micro pollutants, macroscopic impurities and pathogens have not yet been considered and this requires further evaluation in the future. The P-rich solution could be used as liquid fertilizer or be further processed by adding Calcium to precipitate calciumphosphate. In addition, the iron hydroxide precipitate could possibly be reused in the steel industry or transformed to iron chloride by dissolution in hydrochloric acid. In the last case, the heavy metals in the iron residue may require removal.

Through the magnetic separation and the alkaline treatment, 16–32% of P has been recovered from the digested sludge. This is a promising result for a first proof of concept, the objective of this study, considering that the digested sludge has not been optimized for maximum vivianite formation. Further optimization is needed to increase the P recovery and make this approach economically relevant. Firstly, the vivianite content in the digested sludge needs to be maximized (which was not the case for the NL sludge). Increasing the Fe dosing could convert 70–90% of the P in the digested sludge into vivianite [34] which makes it available for magnetic separation. Secondly, recovery and grade can be improved by using a device in which the magnetic field and the separation matrix can be adjusted (use of rods instead of teeth for instance). The influence of these parameters on the separation efficiency is described in [8].

Not only could this technology allow to recover P as vivianite, but

Table 13
Comparison of the concentration of 5 heavy metals present in the P-rich solutions with typical values for P-Rock and future recovered phosphorus salts legislation (Processed results from Table 8).

Elements (mg/kg of P)*	As	Cd	Cr	Cu	Ni	Pb	Zn
PFC 1(C)1**	87	130	13	3921	649	104	9803
P-rock***	66–94	107–271	536–1993	< 1886	< 186	50–100	< 1864
P-rich solution from NL Conc.	186 ± 11	< 195	< 23	1631 ± 81	180 ± 19	< 22	490 ± 28
P-rich solution from FI Conc.	54 ± 6	< 231	< 31	3298 ± 142	1523 ± 105	< 31	417 ± 39

* These 7 elements have been studied because they are the one that will be regulated by the European commission for the product from recovered P (Joint Research Centre 2018). Hg is missing but the ICP-MS used was no able to measure it.

** The product after post-treatment of the P-rich solution falls into the category of recovered phosphorus salts as described in a proposal from December 2018 (Joint Research Centre 2018). This document refers to heavy metal limits for future Product Fertilizer Categories (PFC's, in this case, PFC 1(C)1: Inorganic Macronutrient Fertilizer) in a proposed and by EP amended revision of the fertilizer Ordinance. A product containing 35% of P_2O_5 is considered as reference in the present study which is the minimum phosphate content for this category. The P content is 15.3% of the weight.

*** Dittrich and Klose [6] give the typical amount of heavy metals in the P-rock from Morocco, which is taken as an indicator in this study considering that the country holds around 70% of the world P-rock. The phosphorus content of these rocks is taken from Tahib [28]. The P content is 13.9% of the weight.

its implementation at WWTP's could reduce the quantity of sludge to dispose of, and increase the heating value of this waste sludge by decreasing its mineral content. First estimates show that these benefits, especially the expected reduction of the sludge volume, are in balance with the investment and operation costs of a magnetic separator [35]. Pilot plant operations will have to further confirm the economic benefits of the approach. A direct land application of this sludge with a lower P content would also be easier considering the limitations of P in soil. Finally, a better control of the vivianite precipitation through Fe dosing could minimize the formation of scaling which is a serious problem for WWTP's. These advantages could help making the process economically viable and, therefore, boost the change to a circular economy for P.

5. Conclusion

Vivianite is the most prominent P sink in digested sewage sludge and can contain between 70 and 90% of the total P provided enough iron is present in the sludge. This study proved for the first time the feasibility of the extraction of this mineral with wet magnetic separation technologies. The separated vivianite had a grade of 50–60% and the recovered P-rich solution presented heavy metals concentrations in line with recovered phosphorus legislation. As a proof of concept this is a promising result, but, additional research and development is necessary to improve the P recovery efficiency, for instance through the increase of the Fe dosed to maximize vivianite formation and the optimization of its magnetic separation from digested sludge.

Acknowledgements

This work was performed in the TTIW-cooperation framework of Wetsus, European Centre Of Excellence For Sustainable Water Technology (www.wetsus.nl). Wetsus is funded by the Dutch Ministry of Economic Affairs, the European Union Regional Development Fund, the Province of Fryslân, the City of Leeuwarden and the EZ/Kompas program of the "Samenwerkingsverband Noord-Nederland". We thank the participants of the research theme "Phosphate Recovery" for their financial support and helpful discussions. A special thanks goes to Kees Langeveld from ICL Fertilizers who was the first to suggest magnetic separation techniques. We also want to express our gratitude to Peter Berkhout and his co-workers for the amazing work in the development and building of the μ-Jones separator. Additionally, we thank Outi Grönfors and Wout Barendregt from Kemira and Stefan Geilvoet from Waterschap Hollandse Delta for valuable support during sludge sampling in Espoo and Dokhaven and for providing valuable information about the treatment parameters of these plants.

Appendix A

The Fe/P molar ratio increases after digestion partly due to extra iron added just before digestion in Dokhaven. For Espoo iron-rich secondary sludge was sampled and combined with primary settled sludge in the digester which explains this increase (see Table A1).

Characteristics of both sludges are given in Table A2. It is interesting to notice that the molar Fe/P ratio decreases of ~10% after sieving. The pH has been measured by potentiometry while Total Solid (TS) and Volatile Solid (VS) have been determined following standard methods [39]. Total P and Fe concentration have been determined by ICP-OES after HNO_3-assisted microwave digestion.

Table A1
Characteristics of the studied WWTP's (data from Wilfert et al. 2017).

WWTP	Fe dosing strategy	Solid Retention Time (days)			Fe/P molar ratio		Capacity (p.e. in 150 g TOC/day)
		A-stage	B-stage	Digester	Before digestion	After digestion	
Dokhaven (AB plant)	Fe (III) salts in A-stage	0.3	5.5	35	0.85	1.07	564,000
Espoo (standard CPR)	Fe (II) salts	6–10 (1 step)		13–14	2.19	2.40	321,045

Table A2
Characteristics of the sieved sludges used in the experiments.

Parameter	Netherland	Finland
pH	7.6	7.3
TS (g/kg sludge)	22.2	24.2
VS (g/kg sludge)	14.1	13.8
Total P concentration (mg P/ kg sludge)	57.9	30.2
Total Fe concentration (mg Fe/ kg sludge)	103.0	119.2
Molar Fe: P ratio	0.99	2.19

Appendix B

There are two basic phenomena that determine the separation of magnetic particles from the slurry. First of all, the particles need to reach the teeth as the sludge is poured into the μ-Jones, and then they need to stick to it without being dragged by the slurry. In our experiments, the average velocity for particles of 10–100 μm of diameter (hypothesis based on the authors SEM-EDX observations) toward the magnetic plate of the separator is 3 mm/s. This is high enough to reach the teeth for a classic residence time of a few seconds. Secondly, once attached, the particles need to stick to the wall without being dragged by the slurry. By studying the forces applying on a magnetic particle attached to the teeth, it is possible to determine the maximum feeding flow rate to use before detaching them. The following calculations indicate that a flow rate lower than 28.2 mL shouldn't detach vivianite particles bigger than 10 μm.

Detailed calculations

As the slurry flows along the surface at high magnetic gradient, the paramagnetic particles in the slurry are attracted towards the surface by a force

$$F_{\text{magnetic}} = \mu_0 \rho_p V_p \chi_p H \nabla H \tag{B1}$$

Here, $\mu_0 = 4\pi 10^{-7}$ Tm/A is a universal constant of the laws of magnetics, H (A/m) is the magnetic field and ∇H (A/m^2) is its gradient. The particle is defined by its density ρ_p (kg/m^3), its magnetic susceptibility χ_p (m^3/kg) and its volume V_p (m^3). As the paramagnetic particles travel towards the surface, they experience a drag force. Since the speed Δv of the particle towards the surface is typically of the order of 1 mm/s or less, and particles are 10–100 μm in diameter, the drag on the particle can be estimated by Stokes' formula:

$$F_{\text{drag}} = 3\pi\eta\Delta v D_p \tag{B2}$$

Here, η (kg/m * s) is the dynamic viscosity of the slurry and D_p (m) is the diameter of the particle. Small fines in a liquid very quickly reach a velocity at which drag and external forces are at equilibrium, and so the equations above can be used to estimate Δv for a spherical particle,

$$\Delta v = \frac{\mu_0 \rho_p D_p^2 \chi_p H \nabla H}{18\eta} \tag{B3}$$

Magnetic susceptibilities of Vivianite nodules were found to vary in the range from 0.8 to 1.7 10^{-6} m^3/kg by Minyuk et al. [16]. Conservatively assuming the lower value, a density for Vivianite of 2300 kg/m^3, and a viscosity of the slurry of twice that of water, $2{\cdot}10^{-3}$ kg/m·s, the speed of 10 μm diameter Vivianite particles towards the surface can be estimated as

$$\Delta v = 6{\cdot}10^{-18}\ \text{A}^{-2}\ \text{m}^4\ \text{s}^{-1}\ H\nabla H \tag{B4}$$

Target slurries contain organic fibers of up to 1 mm length and so the channels for the slurry should leave at least a space of 2 mm between surfaces to avoid blocking. Still, this means that an average field of 10^6 A/m and an average field gradient of $0.5 * 10^9$ A/m^2 (i.e. varying by $0.5 * 10^6$ A/m over 1 mm from the center of the channel towards the surface) would result in a particle speed of 3 mm/s. This is more than enough for all such particle to reach the surface for a typical residence time of one or more seconds. Field conditions like these do not require superconducting magnets or steel wool. They can be met by Jones separators with electromagnets and grooved plates, which has the advantage of low investment cost and simple channel geometries that do not easily block.

Once the magnetic particles have reached the surface, they should stick there and not be carried along the surface by the drag of the slurry. The Reynolds number of the flow in the channels formed by the surface is typically below 100, so the friction of the slurry flow per unit area of the coating of magnetic particles on the surface of the channels is

$$f_{\text{friction slurry}} = \frac{8\eta v}{D} \tag{B5}$$

Here v (m/s) is the velocity of the slurry past the surface and D (m) is the diameter of the channel. The friction of the surface of a particle is proportional to the magnetic force pulling the particle to the surface:

$$F_{\text{friction surface}} = f F_{\text{magnetic}} = f\mu_0 \rho_p V_p \chi_p H \nabla H \tag{B6}$$

Since $F_{\text{friction surface}} > A_p f_{\text{friction slurry}}$, where A_p is the part of the surface covered by a single particle, the magnetic field should be strong enough to fix the magnetic particles to the surface:

$$H\nabla H > \frac{8\eta A_p v}{f\mu_0 \rho_p V_p \chi_p D} \tag{B7}$$

Taking again the values for Vivianite as above, and estimating f = 0.5, while conservatively taking $A_p = 5D_p^2$, we get:

$$H\nabla H > 1.7{\cdot}10^{15}\ \ A^2\ \ m^{-4}\ \ s^1\ \ v \tag{B8}$$

With v ≈ 0.1 m/s, this means that, again, Jones separators will do well.

For a full coating of particles $A_p = 5D_p^2$, is a very conservative estimate, since it would be expected that each particle covers roughly its square diameter of the surface. However, for a single particle sticking from the surface, this estimate is probably more appropriate (Table B1).

Table B1
Forces applying on vivianite depending on the flow rate.

Total flow	Drag + gravity force on particles near the wall (pN)			Magnetic stick force on the wall (pN)		
mL/min	10 µm	20 µm	30 µm	10 µm	20 µm	30 µm
7.8	45	207	525	142	1130	3820
16.2	83	360	869	142	1130	3820
24.0	122	513	1210	142	1130	3820
32.4	160	666	1560	142	1130	3820
40.2	198	819	1900	142	1130	3820

Under all these assumptions, it can be seen in Table B2 that a flow rate lower than 24 mL/min should allow all the particles > 10 µm to stick to the walls of the µ-Jones (ratio < 1). The exact cut-off for these particles is 28.2 mL/min.

Table B2
Ratio of the drag and stick forces depending on the flow rate.

Total flow	Ratio of drag and stick		
mL/min	10 µm	20 µm	30 µm
7.8	0.32	0.18	0.14
16.2	0.59	0.32	0.23
24.0	0.86	0.45	0.32
32.4	1.13	0.59	0.41
40.2	1.40	0.72	0.50

Viability of magnetic separation

Experiments were performed to test the viability of magnetic separation of vivianite from sludge. The four tested flow rates are lower than the 28.2 mL/min cut-off previously determined to be sure that the separation will work and to also separate particles smaller than 10 µm. The separation protocol was the same as described in Section 2 with the difference that the flow rate varied and that the pouring time was 30 s for both sludges.

First of all, the separation works for flow rates below 20 mL/min which is in the expected range obtained by theoretical modeling. Indeed, from a certain flow rate, the drag force exerted by the slurry on a particle stuck on the surface becomes higher than the one retaining it against the wall. Fig. B1 shows that for both sludges the enrichment increases for both Fe and P with the flow rate. This is in line with the expectations since non-magnetic impurities are more likely to be flushed out at higher flow rates. The enrichment shows a saturation around 20 mL/min for the Dutch sludge which is not the case for the Finnish sludge (Fig. B1). The maximum magnetic species may have been extracted from the Dutch sludge while a longer pouring time may be needed for the Finnish sludge. It is in accordance with the higher Fe/P ratio of the Finnish sludge, suggesting that a bigger magnetic fraction, containing siderite ($FeCO_3$), pyrite or/and FeO's, is present.

Aside from the enrichment, the recovery of P and Fe has been measured as well. The recovery decreases with the flow rate for the Finnish sludge for both elements while it remains rather stable for the Dutch feed (Fig. B2). Higher streams reduce the part of non/less-magnetic material susceptible to be retained which explains the behavior of the Finnish sludge. 20 mL/min was the highest flow rate tested and, even though it gave lower recovery, it gave the purest product with lower organic matter content and impurities like calcium, sulfur, and silicon. Determining the quantity of vivianite present in the concentrate is easier with purer sample. Therefore, 20 mL/min have been chosen as the working flow rate.

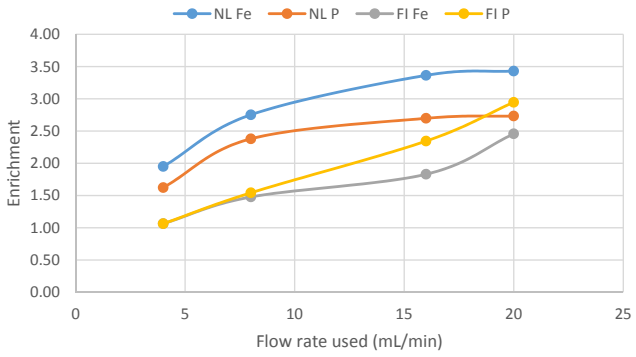

Fig. B1. Enrichment for P and Fe for both sludge at four different flow rates (The enrichment defines the ratio of the weight content of a Fe and P before and after magnetic separation).

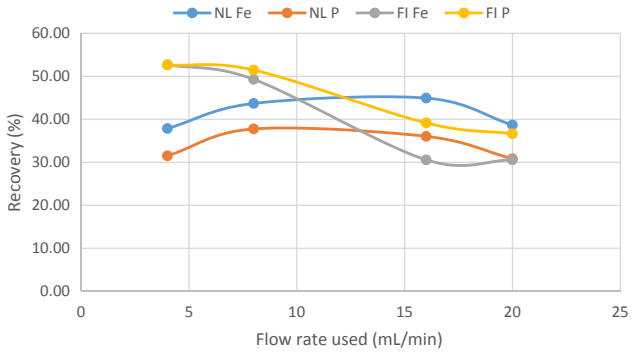

Fig. B2. Recovery of P and Fe for both sludge at four different flow rates.

Appendix C

Carbonate determination

The carbonate content in the sample has been estimated using μGC. First, 20 mg of solid is added to a 25 mL glass vial. 1 mL of HCl 9% (VWR Chemicals) is quickly poured on the powder, and the jar is immediately closed with a rubber stopper. After 10 min, 10 mL of the gas phase is withdrawn and quickly introduced in a μGC for CO_2 determination. The device is a Varian CP 4900 equipped with a Thermal Conductivity Detector. The column used is a PoraPlot U of 10 m long with Helium as a carrier. The data processing is realized with the software GC solution. A blank without any solid but only acid was also prepared.

The quantity of CO_2 released and the quantity of carbonate in the samples are presented in Table C1 (calculation below). There is significantly more carbonate in the samples from Finland (3–5% of dried solid) than the one from the Netherlands (< 1%). Independently from the sludge origin, the share of carbonate seems to decrease after magnetic separation. No CO_2 release has been observed in the case of the scaling sample.

Hypothesizing the total reaction $FeCO_3 + 2HCl \rightarrow FeCl_2 + H_2O + CO_2$, the determination of the carbonate fraction can be done as follow:

$$n_{CO2} = \frac{(X_{CO2} - X_0) \times \rho_{air} \times V_{gas}}{M(CO_2)} \quad \text{(C1)}$$

1 mol of $FeCO_3$ releases 1 mol of CO_2 so:

$$n_{CO2} = n_{FeCO3} \quad \text{(C2)}$$

Giving finally:

$$X_{FeCO3} = \frac{n_{FeCO3} \times M(FeCO_3)}{m_{sample}} \quad \text{(C3)}$$

With:

n_{CO2} the amount of substance of CO_2 released in the tube in moles
X_{CO2} the CO_2 weight fraction of the gaseous phase in the tube
X_0 the CO_2 weight fraction of the blank
ρ_{air} the density of air worth 1.20 g/L at the experimental conditions (20 °C at sea level)
V_{gas} the total volume of the gaseous phase in the tube worth 0.0240 L (1 mL of HCl in 25 mL tube)
$M(CO_2)$ the molar weight of CO_2 worth 44.0 g/mol
n_{FeCO3} the amount of substance of $FeCO_3$ in the sample in moles
X_{FeCO3} the $FeCO_3$ weight fraction of the solid
$M(FeCO_3)$ the molar weight of $FeCO_3$ worth 115.8 g/mol
m_{sample} the weight of the sample introduced into the tube in g

Table C1
Percentage of carbon dioxide evolution and $FeCO_3$ content assuming all evolved carbon dioxide was associated to $FeCO_3$.

Sample	X_{CO2} (%)	X_{FeCO3} (%)
Blank	0.06	0.00
FI Feed	1.33 ± 0.01	4.94 ± 0.04
FI Conc.	0.95 ± 0.03	3.33 ± 0.16
NL Feed	0.25 ± 0.01	0.60 ± 0.03
NL Conc.	0.13 ± 0.01	0.26 ± 0.02
Scaling	0.06	0.00

Quartz determination

It has been noticed that when a sufficient quantity (50 mg) of feed or concentrate is digested, an insoluble white solid remains. Quartz (SiO_2) is hard, or even impossible, to degrade with standard acid digestion. The solid fraction remaining after digestion was carefully collected by centrifugation and dried at 105 °C.

The undigested solid after digestion was isolated and analyzed by SEM-EDX. Si and O were the main components of the sample (> 80% of total weight) in a ratio close to the one of SiO_2. However, there were some other elements homogeneously distributed ranging from Na, Al and Ca at high concentration, to Fe, P, and Cu at minor concentration. The dry weight of the digestion residue was assumed to be entirely quartz for the calculations (Table C2).

Table C2
Digestion residue (assumed to be quartz) content in both sludges.

Sample	Average (% of vacuum dried matter)
FI Feed	8
FI Conc.	8
NL Feed	4
NL Conc.	7

Appendix D

The analytical method chosen for each element as well as the isotope measured is the one recommended by the supplier (Table D1). When gases are used, they are introduced through the skimmer cone (iCRC system) and not in a reaction chamber which is usually the case. Sample collection was done by a FAST 4DX autosampler, from supplier ESI, combined with a FAST collection loop of 1 mL. This allowed rinsing of the uptake tubes, while the sample was simultaneously analyzed from the loop. All the sample, as well as the rinse solution, were prepared with ultra-pure HNO_3 from Fluka and the sample with ultra-pure water from Sigma-Aldrich. The acid content was 4% for all solutions to increase the concentration of traces elements at a maximum. Together with the samples, a blank is prepared by digesting a sample of ultra-pure water only, in the same temperature and acid conditions than with a solid sample.

Table D1
Isotopes analyzed and corresponding methods according to standard settings.

Analytical mode	Isotope analyzed
H_2	^{52}Cr, ^{75}As, ^{78}Se, ^{133}Cs, ^{139}La
He	^{23}Na, ^{56}Fe, ^{85}Rb, ^{140}Ce
ng	^{7}Li, ^{9}Be, ^{11}B, ^{24}Mg, ^{27}Al, ^{29}Si, ^{31}P, ^{34}S, ^{39}K, ^{44}Ca, ^{47}Ti, ^{55}Mn, ^{59}Co, ^{60}Ni, ^{65}Cu, ^{66}Zn, ^{95}Mo, ^{107}Ag, ^{114}Cd, ^{118}Sn, ^{137}Ba, ^{205}Tl, Pb

The calibration curve was realized with standard solutions from Perkin Elmer in 3 different solutions (Table D2) and the concentration used were 0.1/1/5/10/25/50 ppb. These solutions have been prepared in low range to study the elements which concentration cannot be attained with simple ICP-OES. More concentrated elements are not determined here. Result accuracy was checked by analyzing standard reference material 1640a (supplier NIST) at the start and end of the run. The software used for data processing was Aspect MS 4.3.

According to the high NaOH background in the release solution, the samples need to be diluted not to damage the devices. A final concentration of 225 ppm of Na is set to be below the maximum amount of salt allowed of 1000 ppm. The protocol for the experiments stays the same, but with a blank of 225 ppm of Na prepared with ultra-pure water and NaOH. No particular calibration curve has been prepared for samples with NaOH background.

Table D2
Composition of the standard solutions used for calibration of the ICP-MS.

Standard solution	Elements present
1	Ag, Li, Mo, Si, Sn, Tl
2	As, B, P, S, Se
3	Al, Ba, Be, Ca, Cd, Ce, Co, Cr, Cs, Cu, Fe, K, La, Mg, Mn, Na, Ni, Pb, Rb, Zn

Appendix E

.

Table E1a
Elemental composition of the feeds, concentrates and scaling measured by ICP-MS/OES.

Sample	Weight content (g element/kg of P)											
	Cr	As	La	Li	Mg	Al	Mn	Co	Ni	Cu	Cd	Ca
FI Feed	1.17 ± 0.02	0.31 ± 0.02	1.06 ± 0.01	0.13 ± 0.01	141 ± 4*	215 ± 4*	8.86 ± 0.02	0.31 ± 0.01	1.17 ± 0.01	13.31 ± 0.15	nd	940 ± 21*
FI Conc.	0.39 ± 0.07	0.12 ± 0.01	0.38 ± 0.01	0.05 ± 0.01	43 ± 2*	71 ± 2*	6.42 ± 0.05	0.14 ± 0.01	6.17 ± 0.02	15.48**	nd	265 ± 10*
NL Feed	1.36 ± 0.02	1.07 ± 0.03	0.25 ± 0.01	0.10 ± 0.01	91 ± 3*	160 ± 3*	17.0 ± 0.12	0.16 ± 0.01	1.13 ± 0.01	18.34 ± 0.29	nd	968 ± 19*
NL Conc.	0.77 ± 0.02	0.23 ± 0.01	0.09 ± 0.01	0.05 ± 0.01	97 ± 2*	60 ± 2*	31.09**	0.11 ± 0.01	1.17 ± 0.01	9.20 ± 0.05	nd	259 ± 6*
Scaling	nd	nd	nd	nd	91 ± 1*	2.50 ± 0.01	25 ± 1*	0.27 ± 0.01	0.66 ± 0.01	0.14 ± 0.01	nd	80 ± 5*

nd: no data, meaning below LOQ of both ICP.
er.: the ICP-MS device gave an inexplicable error.
* Results from ICP-OES.
** Results from ICP-OES with the element found only in one replicate.

Table E1b
Elemental composition of the feeds, concentrates and scaling measured by ICP-MS/OES.

Sample	Weight content (g element/kg of P)											
	Zn	Mo	Ag	Sn	Ba	Pb	Na	Si	K	S	Rb	Ce
FI Feed	25.51 ± 0.38	0.21 ± 0.01	0.10 ± 0.01	0.96 ± 0.01	4.02 ± 0.02	0.54 ± 0.01	106.91 ± 1.72	278 ± 4*	380 ± 11*	303 ± 4*	0.37 ± 0.01	2.63 ± 0.03
FI Conc.	6.42 ± 0.01	0.06 ± 0.01	nd	0.24 ± 0.01	1.46 ± 0.01	0.13 ± 0.01	nd	85 ± 4*	30.96**	93 ± 13*	0.1 ± 0.01	0.80 ± 0.01
NL Feed	35 ± 3*	0.32 ± 0.01	0.19 ± 0.01	0.68 ± 0.01	10.73 ± 0.03	3.03 ± 0.05	192.51**	187 ± 3*	275 ± 3*	558 ± 6*	0.21 ± 0.01	0.35 ± 0.01
NL Conc.	8.39 ± 0.09	0.07 ± 0.01	0.04 ± 0.01	0.23 ± 0.01	3.11 ± 0.02	1.05 ± 0.01	3.1 ± 0.53	72 ± 2*	23.32**	124 ± 6*	0.06 ± 0.01	0.15 ± 0.01
Scaling	2.25 ± 0.02	nd	nd	nd	nd	0.03 ± 0.01	nd	nd	nd	14 ± 7*	nd	nd

nd: no data, meaning below LOQ of both ICP.
er.: the ICP-MS device gave an inexplicable error.
* Results from ICP-OES.
** Results from ICP-OES with the element found only in one replicate.

Appendix F

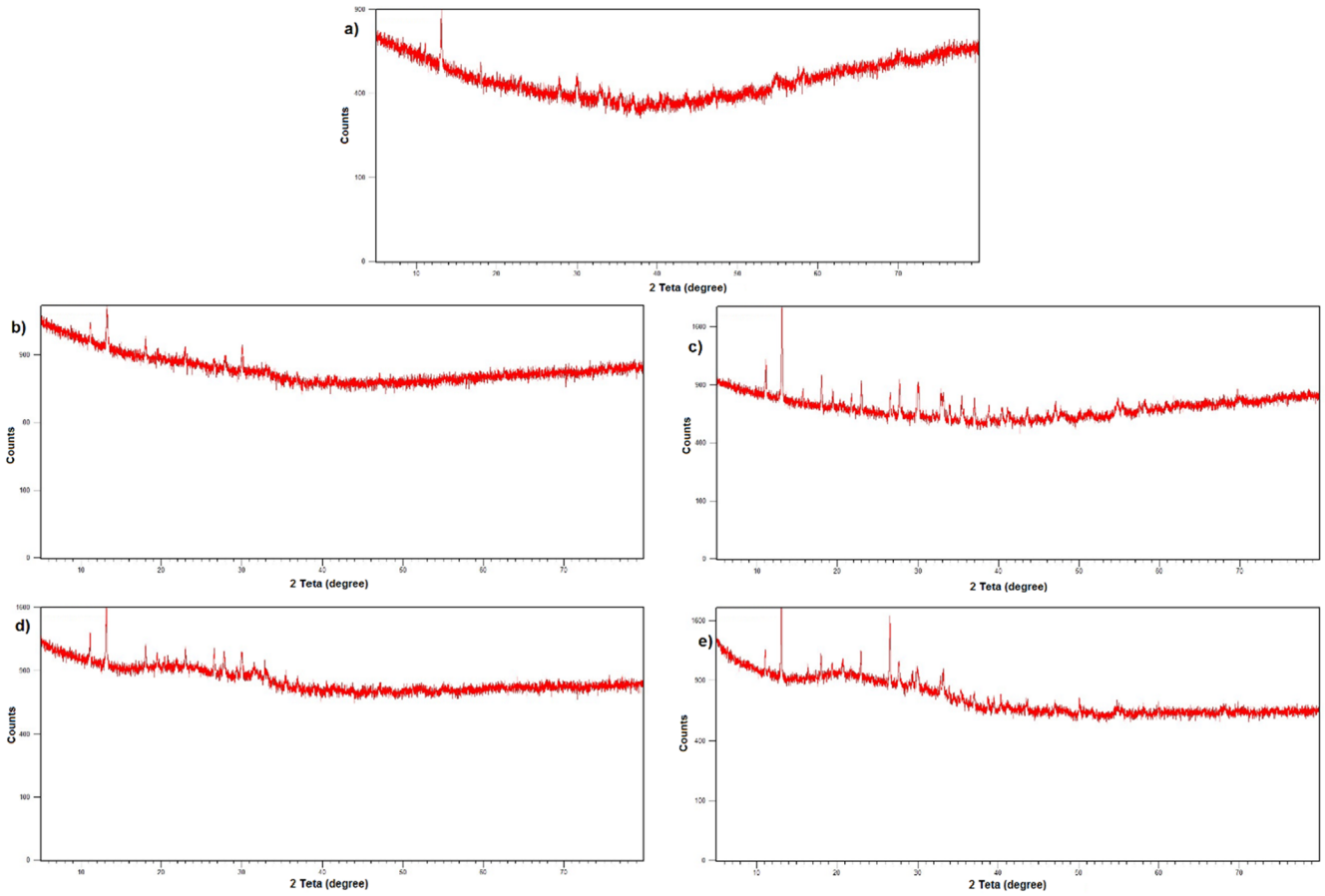

Fig. F1. XRD diffractogram for (a) the scaling, (b) Conc. FI, (c) Conc. NL, (d) Feed FI and (e) Feed NL.

References

[1] E. Barrado, F. Prieto, J. Ribas, F.A. Lopez, Magnetic separation of ferrite sludge from a wastewater purification process, Water Air Soil Pollut. 115 (1) (1999) 385–394.

[2] A. Bouderbala, Magnetic separation of vivianite from sewage sludge, Master's thesis realized at Wetsus in cooperation with the Paris Region Institut for Applied Science Institut Francilien des Sciences Appliquées, 2016.

[3] Z. Čermáková, S. Švarcová, D. Hradil, P. Bezdicka, Vivianite: a historic blue pigment and its degradation under scrutiny, Sci. Technol. Conserv. Cult. Herit. (2013) 75–78.

[4] D. Childers, J. Corman, M. Edwards, J. Elser, Sustainability challenges of phosphorus and food: solutions from closing the human phosphorus cycle, Bioscience 61 (2) (2011) 117–124.

[5] P. Cornel, C. Schaum, Phosphorus recovery from wastewater: needs, technologies and costs, Water Sci. Technol. 59 (6) (2009) 1069–1076.

[6] B. Dittrich, R. Klose, Schwermetalle in Düngemitteln 3 Landesamt Für Umwelt, Landwirtschaft Und Geologie, 2008.

[7] L. Egle, H. Rechberger, J. Krampe, M. Zessner, Phosphorus recovery from municipal wastewater: an integrated comparative technological, environmental and economic assessment of P recovery technologies, Sci. Total Environ. 571 (2016) 522–542.

[8] J. Finch, B.A. Wills, Chapter 13: Magnetic and Electrical Separation, eighth ed., Wills Mineral Processing Technology, 2015.

[9] Y. Fodoué, J.P. Nguetnkam, R. Tchameni, S.D. Basga, J. Penaye, Assessment of the fertilizing effect of vivianite on the growth and yield of the bean "phaseolus vulgaris" on oxisoils from Ngaoundere, Int. Res. J. Earth Sci. 3 (4) (2015) 18–26.

[10] T. Frederichs, T. von Dobeneck, U. Bleil, M.J. Dekkers, Towards the identification of siderite, rhodochrosite, and vivianite in sediments by their low-temperature magnetic properties, Phys. Chem. Earth. 28 (16–19) (2003) 669–679.

[11] E. Frossard, J.P. Bauer, F. Lothe, Evidence of vivianite in $FeSO_4$-flocculated sludges, Water Res. 31 (10) (1997) 2449–2454.

[12] M. Grodzicki, G. Amthauer, Electronic and magnetic structure of vivianite: cluster molecular orbital calculations, Phys. Chem. Miner. 27 (10) (2000) 694–702.

[13] Z. Klencsár, Mössbauer spectrum analysis by evolution algorithm, Nucl. Instrum. Methods Phys. Res., Sect. B 129 (4) (1997) 527–533.

[14] P.G. Manning, T.P. Murphy, E.E. Prepas, Intensive formation of vivianite in the bottom sediments of mesotrophic Narrow Lake, Alberta, Can. Mineral. 29 (1991) 77–85.

[15] C.A. McCammon, R.G. Burns, The oxidation mechanism of vivianite as studied by Mossbauer spectroscopy, Am. Mineral. 65 (3–4) (1980) 361–366.

[16] P.S. Minyuk, T.V. Subbotnikova, L.L. Brown, K.J. Murdock, High-temperature thermomagnetic properties of vivianite nodules, Lake El'gygytgyn Northeast Russia, Clim. Past 9 (1) (2013).

[17] H. Mori, T. Ito, The structure of vivianite and symplesite, Acta Crystallogr. 3 (1) (1950) 1–6.

[18] Y. Nishihara, S. Ogawa, Mössbauer study of ^{57}Fe in the pyrite-type dichalcogenides-isomer shift of divalent iron in low spin state, Le Journal de Physique Colloques 40 (C2) (1979).

[19] J.O. Nriagu, C.I. Dell, Diagenetic formation of iron phosphates in recent lake sediments, Am. Mineral. 59 (1974) 934–946.

[20] M.S. Poffet, K. Käser, T.A. Jenny, Thermal runaway of dried sludge granules in storage tanks, CHIMIA Int. J. Chem. 62 (1) (2008) 29–34.

[21] N. Recham, M. Armand, L. Laffont, J.-M. Tarascon, Eco-efficient synthesis of $LiFePO_4$ with different morphologies for Li-ion batteries, Electrochem. Solid-State Lett. 12 (2) (2009) A39–44.

[22] M. Ridder, S. de Jong, J. Polchar, S. Lingemann, Risks and Opportunities in the Global Phosphate Rock Market, PDF document, 2012. Available at: http://www.phosphorusplatform.eu/images/download/HCSS_17_12_12_Phosphate.pdf Consulted on the 06/06/2018.

[23] A.D. Rombolà, M. Toselli, J. Carpintero, M. Quartieri, J. Torrent, B. Marangoni, Prevention of iron – deficiency induced chlorosis in Kiwifruit (Actinidia deliciosa) through soil application of synthetic vivianite in a calcareous soil, J. Plant Nutr. 26 (10–11) (2007) 2031–2041.

[24] M. Rothe, A. Kleeberg, M. Hupfer, The occurrence, identification and environmental relevance of vivianite in waterlogged soils and aquatic sediments, Earth Sci. Rev. 158 (2016) 51–64.

[25] D. Rouzies, J.M.M. Millet, Mossbauer study of synthetic oxidized vivianite at room-temperature, Hyperfine Interact. 77 (1–2) (1993) 19–28.

[26] O.F. Schoumans, F. Bouraoui, C. Kabbe, O. Oenema, K.C. van Dijk, Phosphorus management in Europe in a changing world, Ambio 44 (2) (2015) 180–192.
[27] A. Seitz, J. Riedner, K. Malhotra, J. Kipp, Iron-phosphate compound identification in sewage sludge residue, Environ. Sci. Technol. 7 (4) (1973) 354–357.
[28] M. Taib, The mineral industries of Morocco and Western Sahara, U.S. Geol. Surv. Miner. Yearb. (2014) 59.1–59.13.
[29] K.G. Taylor, K.A. Hudson-Edwards, A.J. Bennett, V. Vishnyakov, Early diagenetic vivianite ($Fe_3(PO_4)_2$*$8H_2O$) in a contaminated freshwater sediment and insights into zinc uptake: A μ-EXAFS, μ-XANES and Raman study, Appl. Geochem. 23 (6) (2008).
[30] Test Methods for Evaluating Solid Waste, Physical/Chemical Methods, EPA Publication SW-846, third ed. Final Updates V (2015), Method 60-10-D.
[31] K.C. Van Dijk, J.P. Lesschen, O. Oenema, Phosphorus flows and balances of the European Union Member States, Sci. Total Environ. 542 (2016) 1078–1093.
[32] P. Wilfert, P.S. Kumar, L. Korving, G.J. Witkamp, M.C.M. Van Loosdrecht, The relevance of Phosphorus and iron chemistry to the recovery of phosphorus from wastewater, Environ. Sci. Technol. 49 (16) (2015).
[33] P. Wilfert, A. Mandalidis, A.I. Dugulan, K. Goubitz, L. Korving, H. Temmink, G.J. Witkamp, M.C.M. Van Loosdrecht, Vivianite as an important iron phosphate precipitate in sewage treatment plants, Water Res. 104 (2016) 449–460.
[34] P. Wilfert, L. Korving, I. Dugulan, K. Goubitz, G.J. Witkamp, M.C.M. Van Loosdrecht, Vivianite as the main phosphate mineral in digested sewage sludge and its role for phosphate recovery, Water Res. 144 (2018) 312–321.
[35] P. Wilfert. Thesis: Phosphate recovery from sewage sludge containing iron phosphate, 2018b.
[36] B.A. Wills, T.J. Napier-Munn, Will's Mineral Processing Technology: An Introduction to the Practical Aspects of Ore Treatment and Mineral Recovery, 2006.
[37] X. Yang, X. Wu, H. Hao, Z. He, Mechanisms and assessment of water eutrophication, J. Zhejiang Univ. Sci. B 9 (3) (2008) 197–209.
[38] J.L. Zelibor, F.E. Senftle, J.L. Reinhardt, A proposed mechanism for the formation of spherical vivianite crystal aggregates in sediments, Sed. Geol. 59 (1–2) (1988) 125–142.
[39] APHA, AWWA and WEF, Standard Methods for the Examination of Water and Wastewater. 20th Edition, APHA, AWWA and WEF, Washington DC, 1998.